Anal. Chem. **2008,** *80,* 1988−1994

Separation of Bioconjugated Quantum Dots Using Capillary Electrophoresis

Glorimar Vicente and Luis A. Colón*

Department of Chemistry, Natural Science Complex, University at Buffalo, The State University of New York, Buffalo, New York 14260-3000

Capillary electrophoresis (CE) with laser-induced fluorescence (LIF) detection was used to separate different bioconjugated CdSe/ZnS quantum dots (QDs). The QD nanocrystals studied were conjugated to the biomolecules streptavidin, biotin, and immunoglobulin G. The bioconjugated QDs showed different electrophoretic mobilities, which appear to depend upon the biomolecule that is attached to the QD and the buffer solution used. The use of a polymeric additive into the CE run buffer improved the resolution of the bioconjugates. Under CE conditions, the interaction between QD bioconjugates containing streptavidin (QDSt) and biotin (QDBi) was monitored. Under a given set of experimental conditions, the fluorescence intensity of QDSt and QDBi emitting light at 655 nm indicated that about 90% of QDBi complexed with 70% of QDSt. A two-color experiment that made use of two different sizes of QD (i.e., 585 and 655 nm) indicated that 30% of the 655 nm QDBi complexed with 53% of the 585 nm QDSt. The use of QDs with different emission properties allows the selective monitoring of two different wavelengths while using one single excitation source. This, in turn, allowed the monitoring of overlapping peaks in the electropherogram when newly formed products resulting from the interaction of the two bioconjugated QDs appeared.

Bioconjugation of nanoparticles has recently gained popularity in bioanalysis since the nanoparticles can provide unique optical and/or magnetic properties that can facilitate detection and/or identification of biomolecules. One type of such nanoparticles includes semiconductor nanocrystals, also known as quantum dots (QDs), which have been studied widely because of their size-dependent optical properties. These nanoparticles are typically less than 10 nm in diameter and have shown tremendous potential as sensors,[1] optical devices,[2] and as biological labels.[3−6] Furthermore, molecular targets can be encoded with QDs for their specific identification.[3−6] QDs, in principle, could be used in many applications in which organic fluorophores are used. These fluorescent nanoparticles are good candidates for molecular labeling because they are extremely photostable, show broad absorption spectra, narrow emission bands, and are brighter than traditional organic fluorophores.[7,8] Because of the broad absorption spectral characteristics, a single excitation source can be used to excite multiple QDs with different emission spectra, hence, offering the potential of detecting multiple targets simultaneously in a single sample. One can also envision the use of highly efficient separation technology for the separation of nanoparticles bonded to the target molecules from the nonbonded ones.

Capillary electrophoresis (CE) is a powerful separation technique that has been very useful in the analysis of biological samples as it has provided for methods with high selectivity, low detection limits, small sample consumption, ease of use, high separation efficiencies, and short analysis times.[9] CE has found great applicability in the analysis of a variety of biologically important molecules.[10] CE has also been utilized to separate nanomaterials having different compositions and sizes, including latex,[11] inorganic oxide,[12] gold,[13] and silver[14] nanoparticles. Despite the potential advantages of employing QDs as fluorescent labels in combination with CE, just a few reports have appeared in the literature. Huang et al. separated CdTe QDs conjugated to bovine serum albumin from the unconjugated QD using CE/LIF.[15] In a similar study, the authors probed the surface modification of CdTe QDs with two different proteins (plant lectin and anti-von Willebrand factors antibody) using CE.[16] In another study, CdTe QDs of different sizes (1.9 and 4.5 nm) were separated by capillary gel electrophoresis.[17] More recently, Feng et al. developed an immunoassay for the determination of immunoglobulin M using an

* To whom correspondence should be addressed. E-mail: lacolon@buffalo.edu.

(1) Nazzal, A. Y.; Qu, L. H.; Peng, X. G.; Xiao, M. *Nano Lett.* **2003**, *3*, 819−822.
(2) Brus, L. *Appl. Phys. A* **1991**, *53*, 465−474.
(3) Larson, D. R.; Zipfel, W. R.; Williams, R. M.; Clark, S. W.; Bruchez, M. P.; Wise, F. W.; Webb, W. W. *Science* **2003**, *300*, 1434−1436.
(4) Chan, W. C. W.; Nie, S. M. *Science* **1998**, *281*, 2016−2018.
(5) Cognet, L.; Tardin, C.; Boyer, D.; Choquet, D.; Tamarat, P.; Lounis, B. *Proc. Natl. Acad. Sci. U.S.A.* **2003**, *100*, 11350−11355.
(6) Gao, X. H.; Nie, S. M. *Trends Biotechnol.* **2003**, *21*, 371−373.
(7) Smith, A. M.; Nie, S. M. *Analyst* **2004**, *129*, 672−677.
(8) Murphy, C. J. *Anal. Chem.* **2002**, *74*, 520A−526A.
(9) Weinberger, R. *Practical Capillary Electrophoresis*; Academic Press: San Diego, CA, 2000.
(10) Khaledi, M. G. *High Performance Capillary Electrophoresis*; Wiley: New York, 1998.
(11) Jones, H. K.; Ballou, N. E. *Anal. Chem.* **1990**, *62*, 2484−2490.
(12) Petersen, S. L.; Ballou, N. E. *J. Chromatogr., A* **1999**, *834*, 445−452.
(13) Liu, F. K.; Wei, G. T. *Anal. Chim. Acta* **2004**, *510*, 77−83.
(14) Liu, F. K.; Ko, F. H.; Huang, P. W.; Wu, C. H.; Chu, T. C. *J. Chromatogr., A* **2005**, *1062*, 139−145.
(15) Huang, X. Y.; Weng, J. F.; Sang, F. M.; Song, X. T.; Cao, C. X.; Ren, J. C. *J. Chromatogr., A* **2006**, *1113*, 251−254.
(16) Weng, J. F.; Song, X. T.; Li, L. A.; Qian, H. F.; Chen, K. Y.; Xu, X. M.; Cao, C. X.; Ren, J. C. *Talanta* **2006**, *70*, 397−402.
(17) Song, X. T.; Li, L.; Chan, H. F.; Fang, N. H.; Ren, J. C. *Electrophoresis* **2006**, *27*, 1341−1346.

10.1021/ac702062u CCC: $40.75
Published on Web 02/16/2008

antibody labeled with a CdSe/ZnS QD.[18] Pereira et al. used CE to characterize the charge of two commercially available (sodium mercaptopropionate CdTe/ZnS and carboxylic acid CdSe/ZnS) QDs.[19] All of these reports have shown separation of bioconjugated QDs from nonconjugated ones. The separation of different QDs conjugated to different biomolecules, however, has not been reported. CE separation of differently bioconjugated QDs would be useful since it can provide experimental conditions that would allow the development of CE-based assays (e.g., immunoassays) for the determination of specific analytes. Herein, we report on the development of CE conditions for the separation of QDs conjugated to different biomolecules. We explore the possibility of following reactions between biomolecules attached to QDs. In order to prove the feasibility of our approach, we monitored the reaction of streptavidin and biotin, both conjugated to CdSe/ZnS QDs.

EXPERIMENTAL SECTION

Chemicals and Materials. The bioconjugated CdSe/ZnS quantum dots (655 nm QD streptavidin, 585 nm QD streptavidin, and 655 nm QD biotin conjugates) were obtained from Quantum Dot Corporation (Howard, CA). The concentration of the QD nanoparticles, as received, was reported by the manufacturer to be 2 μM. The QDs were received diluted in a pH 8.3 buffer composed of 50 mM borate, 0.5% bovine serum albumin (BSA), and 0.05% sodium azide (preservative). Stock solutions of QDs were prepared using the QD incubation buffer obtained from Quantum Dot Corporation. The composition of QD incubation buffer was 97% deionized water, 2% BSA, <1% sodium borate, and <0.1% sodium azide with a pH of 8.3. A 655 nm QD antibody conjugation kit, also from Quantum Dot Corporation, was used to conjugate the IgG monoclonal antibody, specific for benzodiazepine (BiosPacific, Emeryville, CA) to the QD nanoparticle. For the CE experiments, QDs were dissolved in the running buffer. QDs stock solutions and the incubation buffer were stored at 4 °C. *N*-(2-Hydroxyethyl)-piperazine-2′-(2-ethanesulfonic acid) (HEPES), boric acid, sodium phosphate monobasic and dibasic, tris(hydroxymethyl)aminomethane (Tris), and sodium borate were purchased from FisherBiotech (Fisher Scientific International, Inc., Hampton, NH). 2-(*N*-Cyclohexylamino)ethanesulfonic acid (CHES) was purchased from Sigma-Aldrich (St. Louis, MO). Poly(ethylene oxide) (MW = 100 000) was purchased from Polysciences, Inc. (Warrington, PA). When needed, buffers were adjusted to the desired pH with a stock solution of 1 M sodium hydroxide. The water used to prepare all solutions was purified using a Milli-Q UV Plus water purification system fed from a Milli-RO 10 Plus reverse osmosis system from Millipore (Bedford, MA).

QD Bioconjugation. Conjugation of QD with the IgG antibody was carried out following the protocol provided in the QD antibody conjugation kit. Briefly, 125 μL of the QD-containing solution was activated using succinimidyl-4-(*N*-maleimidomethyl)-cyclohexane-1-carboxylate (SMCC). Size exclusion chromatography (SEC) using a NAP-5 column was used to remove excess SMCC. Dithioethreitol (DTT) was added to the IgG solution to expose free sulfhydryls, and excess DTT was removed by SEC. Activated QDs were then covalently attached to the reduced IgG by combining both solutions for 1 h before quenching with β-mercaptoethanol. The conjugate was centrifuged and purified using SEC. The concentration of the final purified conjugate was determined to be 1.3 μM by measuring the absorbance of the solution at 638 nm.

Instrumentation. All electropherograms were obtained using a P/ACE MDQ CE system from Beckman-Coulter Instruments (Fullerton, CA). System operation and data collection were controlled using the Beckman P/ACE System, version 2.3 software, also supplied by Beckman-Coulter Instruments. Detection was performed using a laser-induced fluorescence detector (Beckman-Coulter). The excitation source was provided by a Beckman-Coulter 488 nm argon ion laser module. The emitted light was filtered through a 488 nm notch filter before passing through a 655 or 585 nm band-pass filter (Omega Optical, Brattleboro, VT), depending on the emission of the QD used. The detection window was obtained by burning a small section of the polyimide coating followed by a rinse with methanol. Data were acquired at 4 Hz. CE experiments were all performed in 50 μm i.d. × 31 cm long fused-silica capillaries (Polymicro Technologies, Phoenix, AZ). The effective length (i.e., length from injection to the detection window) was 20 cm. Capillaries were conditioned by rinsing for 10 min with 0.1 M NaOH, 10 min with water, and 10 min with the running buffer, before equilibration at the separation voltage prior to analysis. Injection was performed hydrodynamically by applying 0.5 psi typically for 5 s. Separations were carried out at 15−30 kV, while column temperature was maintained at 20 °C. In between runs the capillary was rinsed with 100 mM NaOH for 1 min and with running electrolyte for 1 min. Origin Pro 7.5 (Origin Labs) was used to fit electropherograms to the Gaussian model.

RESULTS AND DISCUSSION

CE/LIF of Bioconjugated QDs. The separation of different bioconjugated QDs by CE in free solution could be expected to be somehow challenging due to their similarities in sizes. As the sizes of the entities to be separated become larger the difference in charge-to-mass ratio becomes negligible making separation by CE in free solution more difficult to perform. The size of the bioconjugated QDs used in this work varied from about 10 nm for the 655 nm biotin conjugated QD (QDBi) to about 15−20 nm for the 655 and 585 nm QDSt; this is including the attached biomolecule (according to the manufacturer). The size of the 655 nm QDIgG bioconjugate derivatized in our laboratory is not known; however, the overall size of the QD bioconjugate is expected to be larger than the QDSt, given the difference in size of the two biomolecules (cf., Table 1).[20] The surface attachment of biomolecules to QDs, however, should impart characteristics of the biomolecule to the nanoparticle. These characteristics can provide for differentiation of the bioconjugated nanoparticles and, hence, separation in the CE system.

The QDs used in our studies were conjugated to biotin (QDBi), streptavidin (QDSt), and to an IgG antibody (QDIgG), having emission at 655 nm. A fourth QD with emission at 585 nm conjugated to streptavidin was also used. All QDs had a core/

(18) Feng, H. T.; Law, W. S.; Yu, L.; Li, S. F. Y. *J. Chromatogr., A* **2007**, *1156*, 75−79.

(19) Pereira, M.; Lai, E. P. C.; Hollebone, B. *Electrophoresis* **2007**, *28*, 2874−2481.

(20) Choi, H. S.; Liu, W.; Misra, P.; Tanaka, E.; Zimmer, J. P.; Ipe, B.; Bawendi, M. G.; Frangioni, J. V. *Nat. Biotechnol.* **2007**, *25*, 1165−1170.

Table 1. Electrophoretic Mobilities of QD Bioconjugates

bioconjugated nanocrystals	biomolecule	molecules/ QD[a]	electrophoretic mobilities $\times 10^{-4}$ (μep, cm^2/V·s)[b,c,d]
655 nm CdSe ZnS QD streptavidin	streptavidin pI = 5−6 MW = 60 000 Da	5−10	−3.86 ± 0.02
585 nm CdSe ZnS QD streptavidin	streptavidin pI = 5−6 MW = 60 000 Da	5−10	−3.56 ± 0.04
655 nm CdSe ZnS QD IgG	IgG pI = 6−7.3 MW = 150 000 Da	1−2	−3.57 ± 0.02
655 nm CdSe ZnS QD biotin	biotin pK_a = 4.51 MW = 244 Da	5−7	−4.57 ± 0.02

[a] Provided by Quantum Dot Corporation. [b] CE conditions: capillary column, 50 μm i.d., 20 cm effective length (30 cm total length); running buffer, 100 mM CHES, pH 9.5; injection, 5 s at 0.5 psi; applied voltage, 20 kV; excitation source, 488 nm argon ion laser; detection, 655 nm band-pass filter (for QDs with emission in 655 nm) and 585 nm band-pass filter (for QD with emission in 585 nm); data collection rate, 4 Hz; capillary temperature, 20 °C. [c] Electroosmotic flow was measured using mesithyl oxide as the neutral marker. Electroosmotic mobility = 6.72×10^{-4} cm^2/V·s. [d] Electrophoretic mobilities were measured in triplicate.

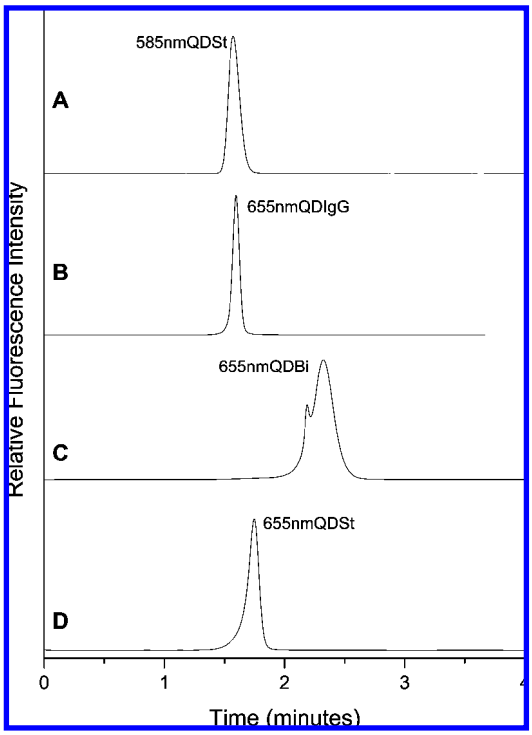

Figure 1. Electropherograms of individual the bioconjugated nanocrystals (A) 585 nm QDSt, (B) 655 nm QDSt, (C) 655 nm QDBi, and (D) 655 nm QDIgG. CE conditions: capillary column, 50 μm i.d., 20 cm effective length (30 cm total length); running buffer, 100 mM CHES, pH 9.5; injection, 4 s at 0.5 psi; applied voltage, 20 kV; LIF detection, λ_{ex} = 488 nm, λ_{em} = 655 nm or 585 nm; data collection rate, 4 Hz; capillary temperature, 20 °C.

shell composed of CdSe/ZnS. We first measured the electrophoretic mobilities of the different QD bioconjugates by injecting each one individually into the CE system under a given set of conditions. Figure 1 shows electropherograms of the individual bioconjugated QDs. The electrophoretic mobilities and other characteristics (i.e., emission wavelength, biomolecule attached, and number of biomolecules per nanocrystal) of the bioconjugated QDs are presented in Table 1. Some characteristics of the molecule attached to the QDs (e.g., molecular weight, isoelectric point, or pK_a) are also provided in Table 1. Under the experimental conditions used, all the QDs tested were negatively charged. Indeed the pH conditions used in the experiments (i.e., pH = 9.5) were favorable to negatively charge the biomolecules attached at the surface of the QDs. The difference in the observed electrophoretic mobilities suggests that the biomolecules attached at the surface of the QDs can provide for electromigration differentiation. The biomolecules attached to the surface of the QDs will have a contribution to both the overall mass and charge of the nanoparticles, thus contributing to the different electromigrations.

In Figure 1, it can be observed that the peaks in the electropherograms for the different bioconjugated QDs are relatively broad. We speculate that the broadening of the peaks may be caused by two factors. First, it could be an indication of the heterogeneity in the size distribution of the QDs. Even though the synthesis of QDs can produce relatively tight narrow size distribution,[21−23] there are always size differences and hence heterogeneity. Such size differences can cause a slightly different migration time of nanoparticles, reflected on the width of the CE peaks. Second, the broadening of the peaks can also be attributed to additional heterogeneity in size introduced by the bioconjugation since the QDs can have different amounts of biomolecules attached to their surfaces. The amount of biomolecules per nanoparticle (see Table 1) as provided by the manufacturer had a range, which indeed indicates heterogeneity in the bioconjugated nanoparticles due to the number of biomolecules attached; these differences can also contribute to the widths of the peaks obtained in the CE experiments.

Separation of Bioconjugated QDs. The difference in electrophoretic mobilities of the bioconjugated QDs suggests that electrophoretic separation is feasible. Figure 2 shows electropherograms for the separation of different bioconjugated QDs. Separation of 655 nm QDBi and 655 nm QDIgG was achieved using 100 mM CHES, pH 9.5, as the running buffer (Figure 2A). Since 655 nm QDSt and 655 nm QDIgG had similar electrophoretic mobilities under the CE experimental conditions, baseline separation was not achieved (Figure 2B). Addition of polymers to the running buffer has improved separation of nanoparticles of the same composition but with different sizes.[24] We explored the effect of adding poly(ethylene oxide) (PEO) in the running electrolyte on the separation of different bioconjugated QDs. Addition of PEO to the 100 mM CHES pH 9.5 run buffer, however, did not improve the separation of 655 nm QDSt and 655 nm QDIgG (data not shown).

(21) Hines, M. A.; Guyot-Sionnest, P. *J. Phys. Chem.* **1996**, *100*, 468−471.
(22) Landes, C.; Burda, C.; Braun, M.; El-Sayed, M. A. *J. Phys. Chem. B* **2001**, *105*, 2981−2986.
(23) Cumberland, S. L.; Hanif, K. M.; Javier, A.; Khitrov, G. A.; Strouse, G. F.; Woessner, S. M.; Yun, C. S. *Chem. Mater.* **2002**, *14*, 1576−1584.
(24) Armstrong, D. W.; Schulte, G.; Schneiderheinze, J. M.; Westenberg, D. J. *Anal. Chem.* **1999**, *71*, 5465−5469.

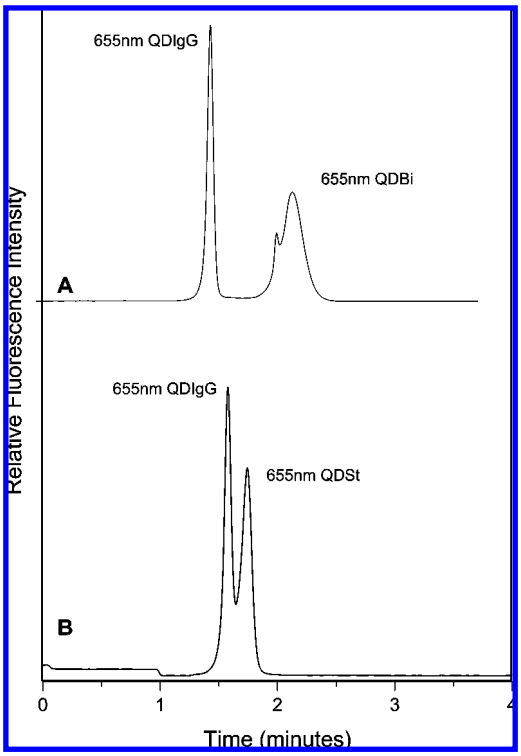

Figure 2. Electropherograms for the separation of (A) 655 nm QDIgG and 655 nm QDBi and (B) 655 nm QDIgG and 655 nm QDSt. CE conditions: capillary column, 50 μm i.d., 20 cm effective length (30 cm total length); running buffer, 100 mM CHES, pH 9.5. Other conditions were as described in Figure 1.

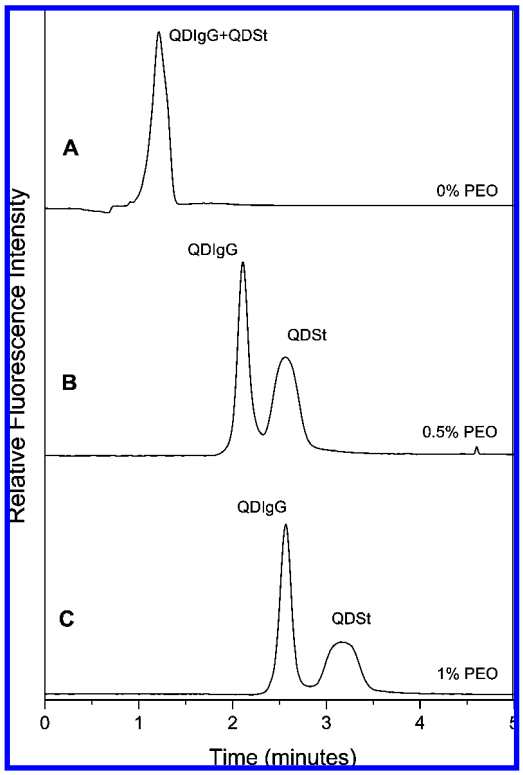

Figure 3. Electropherograms for the separation of 655 nm QDSt and 655 nm QDIgG using different concentrations of PEO in the run buffer: (A) no PEO, (B) 0.5% PEO, and (C) 1.0% PEO. CE run buffer 4.0 mM Tris/4.0 mM borate (pH 8.4). Other separation conditions were as described in Figure 1.

An alternate buffer system in combination with PEO was sought. A buffer system composed of 4.0 mM Tris/4.0 mM borate (pH 8.4) containing PEO proved to be effective in the separation of 655 nm QDSt and 655 nm QDIgG. The influence of the PEO concentration (0−1.0%) in the electrophoretic buffer on the electrophoretic separation is shown in Figure 3. The resolution of the conjugated QDs improved with increasing PEO concentration. PEO has an important role in the separation of these two entities, since separation under these conditions is only obtained when PEO is added to the running buffer. We noticed that the migration time and width of the peaks increased as the polymer concentration was increased. Although the width of both peaks increased with addition of PEO, it is more noticeable with the 655 nm QDSt. The role of PEO in the electrophoretic separation of relatively large species (e.g., micoorganisms) has been discussed previously.[24] A rapid electroosmotic flow (EOF) can minimize the electrophoretic contribution of the QD bioconjugates in the separation. When PEO is added to the run buffer solution, the EOF is decreased, and this allows for an increased electrophoretic contribution of the QD bioconjugates to the separation. In Figure 3, QDSt spends more time inside the column under the influence of the electric field, and as PEO is added the migration time is delayed and the heterogeneity of the nanoparticles also appears to be more noticeable. This effect is more pronounced with the buffer having a slower electroosmotic mobility (Tris−borate shows a slower EOF than CHES buffer).

Interaction of Biotin and Streptavidin QD Conjugates. We explored the possibility of monitoring the interaction of two biomolecules, each attached to a different QD nanoparticle. The biotin−streptavidin system was selected since it is well-known for its stability and affinity; therefore, 655 nm QDBi and 655 nm QDSt conjugates were used. Various buffer systems with and without PEO were studied in order to identify conditions that would provide adequate separation between QDSt and QDBi. Through the optimization, we noticed that the use of different buffers affected the shapes of the peaks in the electropherograms. Interestingly, we observed that some buffer systems (e.g., 100 mM CHES, pH 9.5, 10 mM phosphate, pH 8.0) provided for some differentiation within the distribution of the same QD conjugate (e.g., see Figures 1C and 2A). Such distributions could be attributed to QDs with different sizes and/or different amounts of biomolecules per QD nanoparticle. The addition of PEO to the different buffer systems, however, caused a greater difference in migration time between both conjugates in all buffer systems tested. In addition, adding PEO caused longer overall migration times and broader peaks. A relatively large difference in migration times for the 655 nm QDSt and 655 nm QDBi nanocrystals was observed with the buffer system composed of 4.0 mM Tris/4.0 mM borate (pH 8.4) containing 0.5% PEO. This buffer system, therefore, was selected to monitor the interaction of 655 nm QDSt and QDBi bioconjugates.

An aliquot of 10 μL of 655 nm QDSt (1 nM) was mixed with 10 μL of 655 nm QDBi (1 nM) and allowed to react. The reaction was then followed as a function of time using CE/LIF. The migration times for 655 nm QDSt and 655 nm QDBi when injected separately were 1.68 and 3.02 min, respectively (see Figure 4, parts A and B). If complexation between the two bioconjugated QD proceeded, it would be reasonable to expect a third peak in the

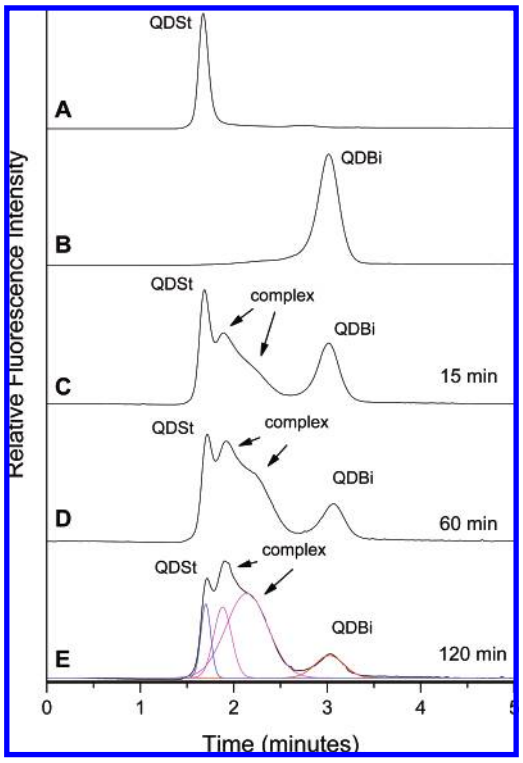

Figure 4. Electropherograms of (A) 655 nm QDSt, (B) 655 nm QDBi and after mixing them for (C) 15, (D) 60, and (E) 120 min. Gaussian fitting of the bands is also included in (E). The run buffer was 4.0 mM Tris/4.0 mM borate, 0.5% PEO (pH 8.4); applied voltage, 30 kV. Other conditions were as described in Figure 1.

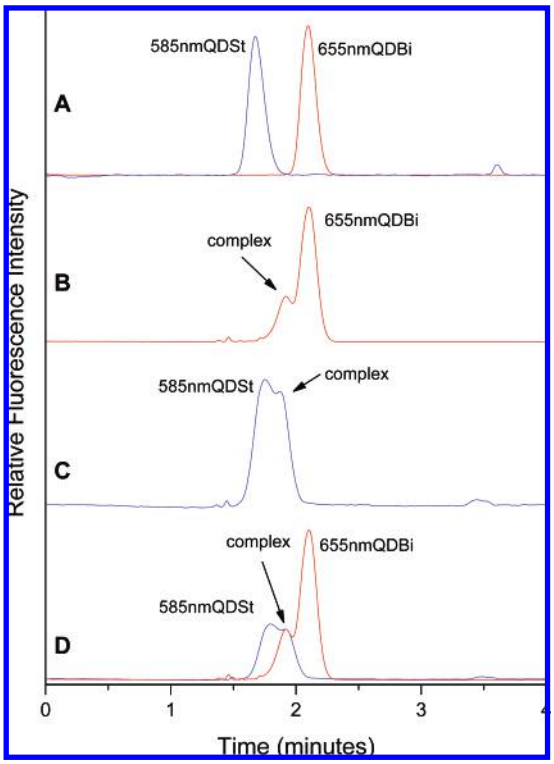

Figure 5. Electropherograms of (A) 585 nm QDSt and 655 nm QDBi (superimposed traces), and after 2 h of mixing monitored at (B) 655 and (C) 585 nm, signal intensities normalized to the total initial intensity of the corresponding unreacted bioconjugated. (D) Superimposed product-normalized traces monitored at the two different wavelengths. CE run buffer: 10 mM borate, 0.5% PEO, pH 9.2; other separation conditions were as described in Figure 1.

electropherogram. Indeed, this is the case; the emergence of a third component is observed in between the migration time for the QDSt and QDBi. Figure 5C−E shows electropherograms of the reaction mixture injected at 15, 60, and 120 min after mixing the bioconjugated 655 nm QDBi and QDSt nanoparticles. From the electropherograms one can observe the growth of a new feature in between the peaks associated with 655 nm QDSt and 655 nm QDBi. As time elapses, it can be seen that the peaks for QDBi and QDSt decreased with a concomitant appearance of the new feature. This new feature is attributed to QDBi−QDSt complex formation. The new band attributed to the complex continued to grow, but after 2 h of reaction no further changes were observed. The new feature in the electropherogram showed a broad distribution that expands between the peaks of the unreacted bioconjugates; this is more prominent after 60 min of mixing the QD bioconjugates. The broadening of the new band can be indicative of multiple interactions between the QDBi and QDSt, leading to more than one distribution of QDBi−QDSt complex formation. Although the new feature in the electropherogram may represent multiple peak distributions, one can identify two major distributions; this becomes more apparent after curve fitting the data related to the reaction for 120 min to the Gaussian model (see Figure 4E).

Each streptavidin can potentially interact with four different biotin molecules. However, because each QD has more than one molecule attached to it, it is unlikely that a streptavidin molecule would bind four biotin molecules, considering the spatial/geometrical constrictions. One can think of the complex(s) as the formation of different clusters of nanoparticles that come together. Therefore, it is reasonable to expect a distribution of clusters having different amounts of particles, which would be reflected in the distribution of migration times. From the peak intensities of the starting materials and after 120 min, 90% of the starting 655 nm QDBi had reacted with 70% of 655 nm QDSt, giving a ratio of 1.3:1 (QDBi/QDSt). We did not observe any interaction of QDBi or QDSt with other QDs (see, for example, Figures 2 and 3). We only observed new features in the electropherogram when QDSt and QDBi were mixed, indicating that the interactions are due to the biomolecules (i.e., St and Bi) attached to the QDs and not to nonspecific interactions between the QDBi and another QD that does not have the streptavidin bioconjugation.

As the 655 nm QDSt and the 655 nm QDBi interacted, the nanoparticle complexes (or clusters) formed led to a very broad band that ran into the bands of the unreacted QD bioconjugates. Although Gaussian modeling of the data can be of help (see Figure 4E), attempting to discriminate among individual components of the complex band distribution and/or from the initial QD reactants can be a difficult task. Instead of using QDs of the same 655 nm color, one can use QDs with different emission wavelengths, while using a single excitation source. In such a case, overlapping peaks can be separated by monitoring each QD at a specific wavelength, which allows for the deconvolution of the overlapping peaks corresponding to reactants and products in the electropherogram. To this end, we mixed two QD bioconjugates having different fluorescence characteristics (i.e., 655 nm QDBi with 585 nm QDSt). These QDs were both excited with a single

excitation source (488 nm argon ion laser) while their respective fluorescence was monitored using a dual-channel detection system. One channel collected the light emitted at 655 nm while the other channel collected the light emitted at 585 nm.

To monitor the interaction of the 585 nm QDSt with the 655 nm QDBi, 10 μL aliquots of each at a concentration near 1nM were mixed. The mixture was allowed to react and injected into the CE system at different intervals. As with the previous reaction a new feature appeared in the electropherogram, this time attributed to 585 nm QDSt−655 nm QDBi complex formation. Figure 5 shows electropherograms of the individual (i.e., unreacted) QD bioconjugates and after mixing for 2 h, monitored at the two different wavelengths. The CE buffer used to monitor the reaction consisted of 10 mM borate, 0.5% PEO, pH 9.2. This buffer composition is different than the one used in the one-color experiment of Figure 4. As previously noted, the use of different buffers had an effect on peak shape and broadening, and some buffer compositions provided for some differentiation even within the distribution of the same QD conjugate. The experimental conditions for Figure 5 provided faster migration times and peaks that did not reflect the partial differentiation within the complex peak. The selection of the appropriate buffer conditions provided adequate resolution between the unreacted bioconjugated QDs and the appearance of only one peak corresponding to the formation of the new product; these all facilitate the deconvolution from the unreacted species (vide infra).

The fluorescence signal intensity collected from each detection channel was normalized to the total initial intensity of its corresponding unreacted bioconjugated QD. In Figure 5A, the electropherograms of the unreacted bioconjugated QDs are superimposed on the same plot. The electropherograms shown in Figure 5, parts B and C, correspond to CE runs monitored at 655 and 585 nm, respectively. The peaks shown in Figure 5B correspond to the unreacted 655 nm QDBi and to the newly formed complex, which contained 585 nm QDSt. The two peaks observed in Figure 5C correspond to the 585 nm QDSt and the complex, which also contained 655 nm QDBi. Clearly, it can be seen that both electropherograms of the mixture containing the QD bioconjugates, monitored at different wavelengths, show overlapping bands that correspond to unassociated QD conjugate and to the product formed from the association of the two different QD bioconjugates. Because the newly formed product contains both QDs, each with a different color, the product is observed at the two different wavelengths monitored. Only one of the unreacted QD bioconjugates, however, is observed in each electropherogram, the one associated with the particular wavelength monitored.

The signal intensity and peak shapes observed in Figure 5, parts B and C, did not change after 2 h of mixing the QD bioconjugates, similar to the experiments with one color. In contrast to what is presented in Figure 4 (one-color experiments), the newly formed feature in the electropherogram appeared as a more defined band. The signal intensity of this new band at each wavelength will depend on how much of the initial bioconjugated QD at that wavelength participated in the complex formation. In our case, after 120 min of reaction, the fluorescence signal intensity shows that 30% of the QDBi appeared to have reacted with 53% of the QDSt, giving a QDBi/QDSt ratio of 1:1.8. This is

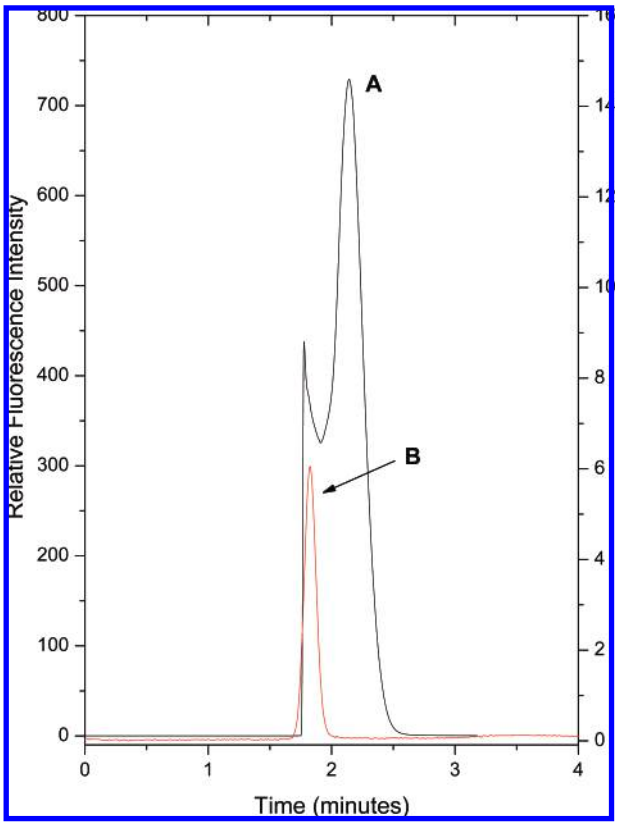

Figure 6. Electropherograms of (A) 655 nm QD biotin (~0.2 μM) and (B) after fraction collection (15 times) of (A); the *y*-axis on the left corresponds to (A) and the *y*-axis on the right corresponds to (B). CE conditions: capillary column, 50 μm i.d., 20 cm effective length (30 cm total length); running buffer, 100 mM CHES, pH 9.5; injection, 3 s at 0.5 psi; applied voltage, 30 kV; other separation conditions were as described in Figure 1.

in contrast with the one-color experiment, where the QDBi/QDSt ratio was 1.3:1. One can attribute this to the different size of the QDSt bioconjugates. Now, the product formed is the same, regardless of the wavelength used for monitoring. Therefore, we can normalize the intensity of the bands in the electropherograms collected at each wavelength to the intensity of the band corresponding to the new product in each electropherogram. This would allow deconvolution of the overlapping bands by superimposing the electropherograms obtained at the two different wavelengths and reconstructing only the band for the new band (i.e., subtracting out the unreacted bands). This is illustrated in Figure 5D, where the normalized signals of the electropherograms shown in Figure 5, parts B and C, are shown superimposed one on the other. If desired, an electropherogram can now be reconstructed for the new band alone by plotting only the nonoverlapping portions of each electropherogram.

In our system, the signal intensity of the product did not any change after 2 h of mixing the two different bioconjugated QDs. Therefore, we assumed that there were no more reactions between QDBi and QDSt. If one desired to monitor the complex formation as a function of time following the approach presented above, it would be more appropriate to normalize all the electropherograms to the signal intensity of the product once it has reached its maximum (i.e., signal intensity of the product does not change with time, indicating that the reaction has reached completion). We want to point out that the interaction between

the conjugated QDs can be monitored by CE because the kinetics of the conjugated QDs interaction is slow relative to the time frame of the CE separation.

Fractionation. Several electropherograms of the bioconjugated QDs showed broad bands, and in some instances peak splitting is observed (see, for example, Figure 1C), particularly under certain buffer conditions. In the case of 655 nm QDBi, we also noticed that peak splitting and broader peaks became more prominent after 6 months of receiving the materials. We explored the potential use of CE to fractionate one of the peaks of the 655 nm QDBi, using 100 mM CHES, pH 9.5, as the CE run buffer. The electropherograms in Figure 6A corresponds to an injection of a sample that clearly showed two different distributions of nanoconjugated QDs. Fraction collection was performed for about 15 times in order to collect enough volume that could be used for reinjection into the CE system, collecting the early eluting fraction of the peak shown in Figure 6A. Figure 6B depicts an electropherogram of the fraction collected, which shows a single peak. One can notice that the migration time of the band in Figure 6B does align well with that of the band at the front end of the major band in Figure 6B. This fractionation approach, however, is very time-consuming since the small volume quantities handled by CE required multiple runs, which requires long times to obtain enough quantities of the isolated band.

CONCLUSION

In the separation of bioconjugated QDs, the migration of the bioconjugates is influenced by the type of biomolecule that is attached to the QD and the buffer solution used. Under our CE conditions, it was possible to monitor the reaction between bioconjugated QDs using CE/LIF, demonstrated here with QD streptavidin and QD biotin. The use of multicolor QDs allows for monitoring CE peaks of overlapping components that may arise from the formation of a new product due to the interaction of the bioconjugates. The reactivity of QDSt and QDBi was dependent on the size (i.e., different color) of the bioconjugated QD. Fraction collection in CE showed potential to fractionate a portion of a band distribution of a bioconjugated QD, but multiple fraction collection is required due to the extremely low volumes used in CE, and this is a very time-consuming process.

Although CE in free solution provided for the successful separation of bioconjugated QDs in our experiments, one must realize that there are limitations in using CE in free solution, as is the case with CE separations of relatively large molecules. As the size of the molecule to be attached at the surface of the QDs increases so does the difficulty for CE separation in free solution. However, similar to the case for large molecules, there are other CE alternatives that can be implemented. For example, the use of CE with a sieving matrix (i.e., capillary gel electrophoresis) can be used in a similar way that is used to separate large proteins. Nonetheless, our results suggest that CE could become an important tool for the characterization of bioconjugated QDs and potentially other conjugated QDs. Our approach can be of interest to those investigating assembly of nanoparticles when there is a need to study interactions between two different conjugated QDs. In addition, the use of QDs with CE has potential in the development of affinity CE assays (e.g., immunoassays),[18] although there are areas that still require improvements. For example, improvement in the heterogeneity of QDs would be beneficial to produce sharper, more efficient peaks. The use of smaller QDs would also benefit their use in the CE format; that, however, would require excitation sources in the UV region.

ACKNOWLEDGMENT

We acknowledge the financial support provided by the National Science Foundation, U.S.A. (CHE 0554677). G.V. acknowledges the Arthur Alfonso Schomburg Graduate Fellowship (University at Buffalo) and the Alliance for Graduate Education and the Professoriate (University at Buffalo) for financial support.

Received for review October 5, 2007. Accepted December 16, 2007.

AC702062U